

Spin densities in parabolic quantum wires with Rashba spin-orbit interaction

Sigurdur I. Erlingsson^{*1,2}, J. Carlos Egues^{1,3}, and Daniel Loss¹

¹ Department of Physics and Astronomy, University of Basel, Klingelbergstrasse 82, CH-4056, Switzerland

² Science Institute, University of Iceland, Dunhagi 3, IS-107 Reykjavik, Iceland

³ Department of Physics and Informatics, University of São Paulo at São Carlos, 13560-970 São Carlos/SP, Brazil

Key words Rashba interaction, quantum wires, spin density

Using canonical transformations we diagonalize approximately the Hamiltonian of a gaussian wire with Rashba spin-orbit interaction. This procedure allows us to obtain the energy dispersion relations and the wavefunctions with good accuracy, even in systems with relatively strong Rashba coupling. With these eigenstates one can calculate the non-equilibrium spin densities induced by applying bias voltages across the sample. We focus on the z -component of the spin density, which is related to the spin Hall effect.

Copyright line will be provided by the publisher

The spin-orbit interaction opens up the possibility to manipulate the electron spin using electrical means, either with applied bias or gate voltage [1]. One manifestation of such electrical spin control is the spin Hall effect [2, 3, 4] where spin currents are created via an interplay between spin-orbit interaction and the applied electric field. When the spin Hall effect is considered in systems with finite transverse size the edges plays an important role. In disordered systems one would expect a building up of spin density (spin accumulation) with opposite sign at the two edges. This picture is not necessarily valid in ballistic systems and the wavefunctions (or wavepackets) themselves become important quantities [5]. The wavefunctions can then be used to calculate the bias voltage induced spin density [6, 7, 8, 9, 10, 11, 12, 13, 14, 15].

In this paper we calculate analytically an approximate eigenspectrum of the Rashba Hamiltonian in a gaussian quantum wire. This allows us to calculate analytically the relevant matrix elements and density of states for each transverse mode in the wire with good accuracy, even for relatively strong spin-orbit coupling. The Hamiltonian for the quantum wire made in a 2DEG with Rashba spin-orbit interaction, for a given wavevector k along the wire, is

$$H = \frac{\hbar^2 k^2}{2m} + \frac{1}{2} m \omega^2 y^2 + \frac{\alpha}{\hbar} (\hbar k \sigma_y - p_y \sigma_x) \quad (1)$$

$$= \frac{\hbar^2 k^2}{2m} + \hbar \omega (a^\dagger a + \frac{1}{2}) + \tau_z \alpha k - \frac{\alpha}{\sqrt{2}\ell} (a^\dagger \tau_+ + a \tau_-) + \frac{\alpha}{\sqrt{2}\ell} (a^\dagger \tau_- + a \tau_+). \quad (2)$$

In Eq. (2) we introduced for convenience new spin matrices where $\tau_z = \sigma_y$ and τ_\pm raises and lowers between the σ_y eigenstates. For positive momenta only states $|k, n, \uparrow\rangle$ and $|k, n+1, \downarrow\rangle$ cross in energy. All other states are separated by at least $\hbar\omega$, which allows us to treat the term proportional to $(a^\dagger \tau_+ + a \tau_-)$ perturbatively in $k_{so}\ell \equiv \alpha/\ell\hbar\omega$. Note that our Hamiltonian is time reversal symmetric (there is no external source of magnetic field). Hence we can focus on the positive k states and use the Kramers relations $\epsilon_{n,s}(k) = \epsilon_{n,-s}(-k)$ and $\psi_{k,n,s}(\mathbf{r}) = \psi_{-k,n,-s}(\mathbf{r})$ to obtain the negative k states.

As mentioned above, for the positive momentum states the perturbative term is

$$V = -\frac{\alpha}{2\sqrt{2}\ell} (\tau_+ a^\dagger + \tau_- a), \quad (3)$$

* Corresponding author: e-mail: sie@raunvis.hi.is, Phone: +354 525 4708, Fax: +354 525 4708

and the non-perturbed Hamiltonian is

$$H_0 = \frac{\hbar^2 k^2}{2m} + \hbar\omega(a^\dagger a + \frac{1}{2}) + \alpha\tau_z k + \frac{\alpha}{\sqrt{2}\ell}(\tau_+ a + \tau_- a^\dagger). \quad (4)$$

We define an effective Hamiltonian $H_{\text{eff}} = e^S H e^{-S}$ which results in

$$H_{\text{eff}} = H_0 + \frac{1}{2}[S, V] + \frac{1}{3!}[S, [S, V]] + o((k_{\text{so}}\ell)^4), \quad (5)$$

with S chosen to fulfill the usual condition $V + [S, H_0] = 0$. The S which satisfies the above requirement is

$$S = \frac{\alpha}{2\sqrt{2}\ell(\hbar\omega + 2\alpha k)}(\tau_+ a^\dagger - \tau_- a) + \frac{\alpha^2}{4\ell^2\hbar\omega(\hbar\omega + 2\alpha k)}\tau_z(a^{\dagger 2} - a^2) + o((k_{\text{so}}\ell)^3). \quad (6)$$

The new terms generated by S in the effective Hamiltonian are

$$\frac{1}{2}[S, V] = \frac{\alpha^2(\tau_z(2a^\dagger a + 1) - 1)}{4\ell^2(\hbar\omega + 2\alpha k)} + \frac{\alpha^3(\tau_+ a a^\dagger a + \tau_+ a^{\dagger 3} + \text{h.c.})}{\sqrt{2}4\ell^3\hbar\omega(\hbar\omega + 2\alpha k)} + o((k_{\text{so}}\ell)^4). \quad (7)$$

The term proportional to $\tau_+ a^{\dagger 3}$ and its hermitian conjugate are perturbative, i.e. they only couple terms which are separated by at least $3\hbar\omega$. Furthermore, one can show that the term $\frac{1}{3}[S, [S, V]]$ in Eq. (5) contains no 'diagonal' terms¹ and thus the corrections to the Hamiltonian, and consequently its eigenenergies, are at most $o((k_{\text{so}}\ell)^4)$. The resulting effective Hamiltonian is thus

$$H_{\text{eff}} = \frac{\hbar^2 k^2}{2m} + \hbar\omega(a^\dagger a + 1/2) + \alpha k\tau_z + \frac{\alpha^2(\tau_z(2a^\dagger a + 1) - 1)}{4\ell(\hbar\omega + 2\alpha k)} - \frac{\alpha}{2\sqrt{2}\ell} \left(\tau_+ a \left(1 - \frac{\alpha^2 a^\dagger a}{4\ell\hbar\omega(\hbar\omega + 2\alpha k)} \right) + \left(1 - \frac{\alpha^2 a^\dagger a}{4\ell\hbar\omega(\hbar\omega + 2\alpha k)} \right) \tau_- a^\dagger \right). \quad (8)$$

The above H_{eff} can be exactly diagonalized using a generalized rotation matrix in spin space

$$U = \begin{pmatrix} \cos(\Theta[\hat{n} + 1]/2) & \frac{\sin(\Theta[\hat{n} + 1]/2)}{\sqrt{\hat{n} + 1}} a \\ -a^\dagger \frac{\sin(\Theta[\hat{n} + 1]/2)}{\sqrt{\hat{n} + 1}} & \cos(\Theta[\hat{n}]/2) \end{pmatrix}, \quad (9)$$

where $\hat{n} = a^\dagger a$ and

$$\cos(\Theta[\hat{n} + 1]) = \frac{\left(\frac{1}{2} - k_{\text{so}}\ell^2 k - \frac{(k_{\text{so}}\ell)^2(\hat{n} + 1)}{2(1 + 2k_{\text{so}}\ell^2 k)} \right)}{\sqrt{\left(\frac{1}{2} - k_{\text{so}}\ell^2 k - \frac{(k_{\text{so}}\ell)^2(\hat{n} + 1)}{2(1 + 2k_{\text{so}}\ell^2 k)} \right)^2 + \frac{(k_{\text{so}}\ell)^2(\hat{n} + 1)}{2} \left(1 - \frac{(k_{\text{so}}\ell)^2(\hat{n} + 1)}{4(1 + 2k_{\text{so}}\ell^2 k)} \right)^2}}. \quad (10)$$

The resulting Hamiltonian $H_{\text{diag}} = U^\dagger H_{\text{eff}} U$ is diagonal in the spin and ladder operators and its eigenenergies for positive k are

$$\varepsilon_{0,\downarrow}(k) = \hbar\omega \left(\frac{1}{2}\ell^2 k^2 + \frac{1}{2} - k_{\text{so}}\ell^2 k - \frac{(k_{\text{so}}\ell)^2}{2(1 + 2k_{\text{so}}\ell^2 k)} \right) \quad (11)$$

$$\varepsilon_{n,\downarrow}(k) = \hbar\omega \left(\frac{1}{2}\ell^2 k^2 + n - \frac{(k_{\text{so}}\ell)^2}{2(1 + 2k_{\text{so}}\ell^2 k)} + \Delta_n(k) \right), \quad n > 0 \quad (12)$$

$$\varepsilon_{n,\uparrow}(k) = \hbar\omega \left(\frac{1}{2}\ell^2 k^2 + (n + 1) - \frac{(k_{\text{so}}\ell)^2}{2(1 + 2k_{\text{so}}\ell^2 k)} - \Delta_{n+1}(k) \right), \quad n \geq 0 \quad (13)$$

$$\Delta_n(k) = \sqrt{\left(\frac{1}{2} - k_{\text{so}}\ell^2 k - \frac{(k_{\text{so}}\ell)^2 n}{2(1 + 2k_{\text{so}}\ell^2 k)} \right)^2 + \frac{(k_{\text{so}}\ell)^2}{2} n \left(1 - \frac{(k_{\text{so}}\ell)^2 n}{4(1 + 2k_{\text{so}}\ell^2 k)} \right)^2}. \quad (14)$$

¹ Here, diagonal refers to $a^\dagger a$, τ_z and also the terms containing $\tau_+ a$ and $\tau_- a^\dagger$.

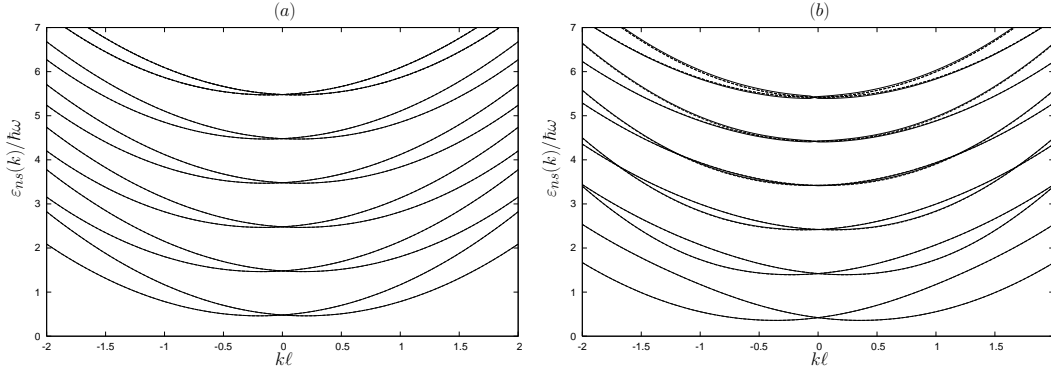


Fig. 1 Energy dispersions of Eqs. (11)-(13) are plotted (solid lines) for the first 6 oscillator levels for $k_{so}\ell = 0.2$ in (a) and $k_{so}\ell = 0.4$ in (b). The dashed lines are the results of numerical calculations. Note that the numerical curves fall on top of the analytical curves except for the highest energy curves in (b).

The negative k branch of the spectrum is obtained from the Kramers relations. In Fig. 1 the energy dispersion for the full spectrum is plotted, along with results of numerical calculations (dashed curves). Even for a relatively large ($k_{so}\ell = 0.4$) perturbation parameter the numerical and analytical curves are barely distinguishable except for the highest transverse states, see Fig. 1b.

Spin densities: Knowing the wavefunctions and eigenenergies allows one to calculate many physical quantities analytically, even non-equilibrium ones. As an example we consider spin densities (transverse to the wire direction) and focus on the the average value of $\sigma_z \delta(y)$. For an applied bias voltage, $\langle \sigma_z \delta(y) \rangle$ is related to the spin-Hall effect [16]. Since the Hamiltonian is time reversal symmetric there will be no equilibrium spin density in the system [17]. Applying a bias voltage lifts this symmetry since Kramers pairs become unequally occupied. For spin densities (and any quantity which is odd under time reversal) only states in the bias window need to be considered. Starting from the non-equilibrium Green's functions[18] it is possible to show that for $kT = 0$ the spin density is

$$\langle \tau_\eta \delta(y) \rangle_{eV} = \sum_{kns} \langle \psi_{kns} | \tau_\eta \delta(y) | \psi_{kns} \rangle \left[f(\varepsilon_{ns}(k) - (\mu + eV)) - f(\varepsilon_{ns}(k) - \mu) \right], \quad (15)$$

where the sum is over all k whose velocity is positive (assuming that $eV > 0$), i.e. the sum contains not only $k > 0$ states but can also include negative momentum states. Although the bias induced spin densities are known analytically through the wavefunctions, the equations are quite long and complicated. As an example we give the following matrix element

$$\begin{aligned} \langle \psi_{kn\uparrow} | \tau_x \delta(y) | \psi_{kn\uparrow} \rangle &= -\sin(\Theta[n+1]) \phi_n(y) \phi_{n+1}(y) \\ &+ \frac{k_{so}\ell}{1 + 2k_{so}\ell^2 k} \left\{ \cos(\Theta[n+1]/2)^2 \phi_n(y) \phi_{n-1}(y) \right. \\ &\quad \left. - \sin(\Theta[n+1]/2)^2 \phi_{n+1}(y) \phi_{n+2}(y) \right\}, \end{aligned} \quad (16)$$

where $\langle y | n \rangle = \phi_n(y)$ are the harmonic oscillator eigenstates. The matrix element in Eq. (16) has the symmetry property $\langle \psi_{kns} | \sigma_z \delta(y) | \psi_{kns} \rangle = -\langle \psi_{kns} | \sigma_z \delta(-y) | \psi_{kns} \rangle$. This is consistent with the spin-Hall effect phenomenology where the transverse spin current leads to opposite spin polarization at the two edges [16, 5]. This property is a direct result of the parity of the harmonic oscillator states $\phi_n(y)$.

The spin densities (normalized to the wire length) for different values of the chemical potential μ are plotted in Fig. 2, assuming linear response $eV \ll \hbar\omega$. As expected the spin density is odd in y and the highest transverse mode contributes the most due to its density of states being the highest. Note that the

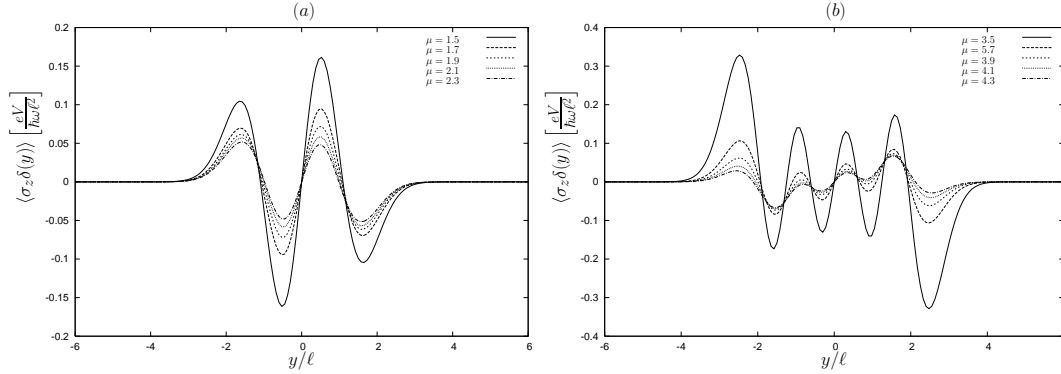


Fig. 2 The spin-density for different μ such that 2 (a), and 4 (b) harmonic oscillator levels for $k_{so}\ell = 0.4$. The spin-density is largest close to each band bottom, where the density of states is greatest.

size of the spin density is comparable to the induced particle density since the matrix element in Eq. (15) is order unity due to the strong coupling of adjacent oscillator states with opposite spin (see Eq. (8))

To summarize, we have calculated the eigenspectrum of a gaussian quantum wire with Rashba interaction. The spectrum allows us to calculate the non-equilibrium spin density analytically. We presented results for the σ_z density for a few low lying oscillator states but the formalism can well handle higher states also.

Acknowledgements This work was supported by the Icelandic Research Fund, the Swiss NSF, the NCCR Nanoscience, EU NoE MAGMANet, DARPA, ARO, ONR, JST ICORP, CNPq, and FAPESP.

References

- [1] *Semiconductor Spintronics and Quantum Computation*, edited by D. D. Awschalom, D. Loss, and N. Samarth (Springer-Verlag, Berlin, 2002).
- [2] J. Sinova, D. Culcer, Q. Niu, N. A. Sinitsyn, T. Jungwirth, and A. H. MacDonald, Phys. Rev. Lett. **92**, 126603 (2004).
- [3] O. Chalaev and D. Loss, Phys. Rev. B **71**, 245318 (2005).
- [4] J. Schliemann, Int. J. Mod. Phys. B **20**, 1015 (2006).
- [5] G. Usaj and C. Balseiro, Europhys. Lett. **72**, 631 (2005).
- [6] M. Lee and C. Bruder, Phys. Rev. B **72**, 045343 (2005).
- [7] A. Reynoso, G. Usaj, and C. Balseiro, Phys. Rev. B **73**, 115342 (2006).
- [8] J. Wang, K. Chan, and D. Xing, Phys. Rev. B **73**, 033316 (2006).
- [9] J. Yao and Z. Yang, Phys. Rev. B **73**, 033314 (2006).
- [10] S. Bellucci and P. Onorato, Phys. Rev. B **73**, 045329 (2006).
- [11] S. DeBald and B. Kramer, Phys. Rev. B **71**, 115322 ((2005)).
- [12] F. Miralles and G. Kircznov, Phys. Rev. B **64**, 024426 (2001).
- [13] L. Serra, D. Sánchez, and R. Lopez, Phys. Rev. B **72**, 235309 (2005).
- [14] M. Governale and U. Zülicke, Phys. Rev. B **66**, 073311 (2002).
- [15] B. Nikolić, L. Zárbo, and S. Welack, Phys. Rev. B **72**, 075335 (2005).
- [16] B. K. Nikolić, S. Souma, L. P. Zárbo, and J. Sinova, Phys. Rev. Lett. **95**, 046601 (2005).
- [17] E. I. Rashba, Phys. Rev. B **68**, 241315R (2003).
- [18] S. Datta, *Electronic Transport in Mesoscopic Systems*, (Cambridge University Press, Cambridge, 1995).